Construction and Building Materials, 254(2020), ARTN 119253.
https://doi.org/10.1016/j.conbuildmat.2020.119253

Cyclic stress-strain rate-dependent response of rubberised concrete

B. Xu[1], D.V. Bompa[1,2*], A.Y. Elghazouli[1]

[1]Department of Civil and Environmental Engineering, Imperial College London, UK

[2]Department of Civil and Environmental Engineering, University of Surrey, UK

Abstract

This paper presents an experimental investigation into the constitutive response of rubberised concrete materials under monotonic and cyclic compression. After describing the test specimens and experimental arrangement, a detailed account of the stress-strain response of rubberised concrete materials, as well as their reference high strength conventional concrete, is given. The volumetric rubber content is varied between 0 and 40% of both fine and coarse aggregates. Both monotonic and cyclic loading conditions are considered for comparison, and three strain rate levels, simulating static, moderate and severe seismic action, are examined. The increase in rubber content is shown to have a detrimental effect on the stiffness and strength, as expected. However, with the increase in rubber content, rubberised concrete materials are shown to exhibit improved compressive recovery under cyclic loading, coupled with a higher energy accumulation rate, enhanced inter-cycle stability and lower inter-cycle degradation. It is also shown that the increase in strain rate, from static to severe seismic, leads to a notable increase in the stiffness and strength, with these enhancements becoming less significant with the increase in rubber content. Based on the results and observations, expressions for determining the unloading stiffness and residual strain, as a function of rubber content and strain rate, are proposed within the ranges considered. The suggested relationships enable the characterisation of rubberised concrete materials within widely used cyclic constitutive models.

Keywords: Rubberised concrete; stress-strain response; cyclic compression; inter-cycle degradation; energy dissipation.

**Corresponding author: Dr. D.V. Bompa; Emails: B. Xu (bowen.xu13@imperial.ac.uk), D.V. Bompa (d.bompa@surrey.ac.uk), A.Y. Elghazouli (a.elghazouli@imperial.ac.uk)*

1 Introduction

The performance of concrete materials provided with recycled tyre rubber particles as a replacement for conventional mineral aggregates has been studied extensively in recent years [1-13]. The proportion replaced influences the fresh, mechanical, physical and long-term properties of rubberised concrete materials (RuC) [1-6]. Compressive and tensile strengths, as well as the elastic and dynamic modulus, decrease with rubber content, whilst the energy dissipation is typically enhanced compared to conventional concrete materials (CCM) [5-10]. Some increase in strength can also often be obtained by rubber particle surface treatment [11]. Earlier work by the authors included extensive compressive tests on unconfined and confined RuC, with volumetric rubber replacement ratio of up to 60%, and led to the development of a full uniaxial constitutive model for RuC under monotonic loading [9,13].

Previous investigations on the cyclic behaviour of structural RuC members have shown the potential benefits in terms of enhanced energy dissipation and damping in comparison to CCM [14-17], but without providing a full characterisation of the cyclic response. It has also been reported that RuC members can absorb up to 2.5 times the energy, with 1.13 times the viscous damping, of their counterparts of CCM members under cyclic loading [15]. When conventional concrete is subjected to loading-unloading cycles, its behaviour exhibits strength and stiffness degradation [18-25], which need to be quantified depending on the type of material. Importantly, most reported tests on the cyclic compressive response of RuC have been limited to rubber content levels below 30%, as a replacement of fine mineral aggregates, which corresponds to a relatively low rubber content of around 11% of the total mineral aggregates [26-29]. Limited studies, on the other hand, investigated the elastic mechanical properties of RuC with relatively high rubber content under cyclic compression or flexural loads [30-37]. However, the fundamental post-peak characteristics of unconfined RuC materials with relatively high rubber content under cyclic compression have not been investigated.

As in monotonic cases, the cyclic compressive strength of concrete materials decreases with the increase in rubber content. The reduction in strength were shown in several studies to be related to the relatively poor bonding between the rubber and the cement [30,31,33,34], while further microstructural investigation indicated that the soft aggregate behaviour of rubber particles increases the porosity of concrete and contributes to the loss in strength [35]. This reduction in strength occurs also due to the lower elastic modulus of rubber particles compared to the replaced mineral aggregates, resulting in elastic incompatibility and stress concentrations and hence

weakness at the interfacial transition zone (ITZ) between the rubber particles and cement matrix [29]. Conventional concrete materials (CCM) are characterised by stiff inclusions, mineral aggregates, in a soft cementitious matrix separated by weak ITZs. Debonding and slip between the inclusions and matrix during cyclic loading, as well as cracks and shear bands in the matrix and inclusions, can contribute to and aggravate the degradation in CCM materials [36-38]. On the other hand, for RuC, particularly when a high rubber content is used, the weaker components would be the rubber particles, and fracture and post-peak degradation would be governed by the rubber-matrix interactions.

In terms of strain rate effects, quasi-brittle heterogeneous materials, such as CCM exhibit rate sensitive characteristics with respect to strength [39]. Both tension and compression strengths typically increase with strain rate and exhibit a critical strain rate beyond which large increases in strength occur [40]. This usually occurs at a rate of about 5 sec^{-1} for tension and 60 sec^{-1} for compression. The initial elastic modulus is normally less sensitive to changes in strain rate than the stiffness and strength around crushing [40]. Moreover, damage accumulation levels were shown to be different for samples subjected to the same stress level, but varying strain rate levels ranging from static (0.5×10^{-5} to 5×10^{-5}) to seismic (1×10^{-4} to 1×10^{-1}) or higher strain levels [40-44]. A number of studies have reported an enhancement in energy dissipation and damping caused by the increase in rubber content [45-54]. On the other hand, there are limited studies on the influence of strain rates on rubberised concrete [55-57]. Due to its hyperelastic nature, rubber is expected to be highly sensitive to strain rates, with significant increase in strength with higher rates. Tests under compression at strain rates above 1×10^{-2} have typically shown that the dynamic increase factors (DIF) for RuC, represented by dynamic-to-static strength ratios, are within those of CCM [55,57], whilst splitting tests have shown that the DIF for RuC are about two folds those of CCM [56,58].

Overall, the addition of rubber particles in concrete have been shown in previous studies to lead to benefits in terms of ductility and energy dissipation. However, fundamental studies on the cyclic response of RuC at strain rates representative of seismic loading have been limited, and have focused on RuC with very low rubber content of up to 11% of the total mineral aggregates or RuC confined properties [26-28]. An in-depth study on the effects of cyclic loading on the mechanical properties and post-peak behaviour of unconfined RuC, including quantification of key constitutive parameters for cyclic stress-strain modelling, is currently lacking. It has already been shown that although the increase in rubber reduces the strength of concrete significantly and, depending on the reference CCM strength, beyond 30-40% rubber the concrete is unlikely to be used in structural elements. However, previous studies on structural members have also shown that the amount of

rubber has little influence on the capacity of flexural members with no or low axial loads [16,59]. It is evident that RuC with reasonable strength, high ductility and energy dissipation can be used in expected plastic hinge zones of flexural members.

To this end, this paper examines the fundamental compression monotonic and cyclic stress-strain properties of unconfined RuC with total rubber content of up to 40%. The experimental investigation considers three strain rate levels representative of static as well as moderate and severe seismic loading. A detailed assessment of the post-crushing energy dissipation, inter-cycle stability and cyclic degradation characteristics of RuC is also included. Based on the results and observations, expressions for determining the unloading stiffness and residual strain, as a function of rubber content and strain rate, are proposed within the ranges considered. The suggested relationships enable the characterisation of RuC materials within widely used cyclic constitutive models.

2 Experimental programme

In total, 90 cylindrical material samples were prepared to assess both the monotonic and cyclic compression behaviour of rubberised concrete (RuC) with various rubber content ratios subjected to three different strain rates (έ). The RuC specimens were prepared by replacing both the fine and coarse aggregates with rubber particles in proportions between 0% to 40% by volume, which correspond to volumetric rubber ratios (ρ_{rv}) in the range of 0 and 0.4, respectively. The volumetric ratio (ρ_{rv}) is the volume of rubber that replaces the mineral aggregates regardless of size and type. The considered strain rates (έ) include: $\acute{\varepsilon}_1=1.67\times10^{-5}$, $\acute{\varepsilon}_2=1.67\times10^{-3}$ and $\acute{\varepsilon}_3=1.67\times10^{-2}$ (sec^{-1}), simulating applied loading rates corresponding to static loading, moderate seismic and severe seismic [43]. Three sets of cylindrical samples (3 × Ø75 mm × 150 mm, where Ø represents the diameter) were prepared for each ρ_{rv} and έ to determine the stress-strain (σ-ε) behaviour for both monotonic and cyclic loading conditions.

2.1 Mix designs and specimen preparation

The sand and gravel used in the RuC mixes were obtained from naturally occurring rock deposits consisting of various mineral contents [60]. The fine aggregates had sizes up to 5 mm with a specific gravity of 2.65 and a moisture ratio of 5%, while the coarse aggregates were of size 5-10 mm, and had a specific gravity of 2.65 and a moisture ratio of 3%. It has been shown that RuC with fine rubber particles has a higher strength as well as lower workability and water permeability than RuC with large particles [11]. To achieve the highest strength possible, whilst incorporating

relatively high rubber volumes (i.e. 40%), fine rubber particles were considered for the mixes in this paper. Complementary admixtures were added and adjusted for each mix to obtain reasonable workability levels, as described below. The rubber particles used in the RuC mixes were acquired from recycled car tyres and manufactured into two size grades of 0.5-0.8 mm and 1.0-2.5 mm as depicted in Figure 1 [61].

The results of a sieve analysis on both mineral aggregates and rubber particles according to EN 933-1 [62] are given in Table 1. CEM I 52.5N was used as the binder in the RuC mixture whilst EN 450-1 [63] fineness category S fly ash and Grade 940 silica fume [64] were also added to improve workability and optimise the particle packing of the mixture. The cement composition contained average ingredients of: 55% Tricalcium Silicate C3S, 20% Dicalcium Silicate C2S, 9.5% Tricalcium Aluminate C3A, 8% Tetracalcium Aluminoferite C4AF, 3.3% Sulfate SO_3, 0.7% Alkali Eq Na_2O, and < 0.1% Chloride [65].

In order to obtain a RuC with reasonable compressive strength and that can be used in practice, for a maximum of 40% rubber content, a relatively high strength CCM is needed. Hence, a reference CCM (R00) with a target strength of 70 MPa was prepared. This had 450kg/m^3 of binders, 60% of which was CEM I 52.5N, 35% was fly ash and 5% was silica fume. It also contained 760 kg/m^3 of sand, 977 kg/m^3 of gravel, 158 L/m^3 of water and 9.5 L/m^3 of superplasticiser [66]. In total, 4 types of RuC mixes were prepared, referred to as R10, R20, R30 and R40, representing 10%, 20%, 30% and 40% replacement of both fine and coarse aggregates with fine rubber. From the reference CCM mix, for R10-R40 concretes, the amount of superplasticiser was adjusted to obtain a mix with reasonable workability. Fresh concrete properties determined by means of a slump cone provided slump values between 105-120 mm for all materials. Although there is no direct match between the gradation curve of the rubber blend comprising 0.5-0.8 mm and 1.0-2.5 mm rubber particles and that of replaced mineral aggregates, the mixes have been designed in relation to the main physical properties of the constituents and visual inspection, as well as slump tests on the fresh mixes, have indicated workable RuC materials. The mix designs of all the RuC materials as well as the reference CCM are given in Table 2. It should be noted that although a drawback of using unconfined high strength concrete as a reference material is its brittle characteristics, this study shows that the inclusion of rubber results in an enhancement of ductility and energy dissipation under cyclic loading.

A rotary mixing machine with a container of 40L was used for all the concrete mixes described herein. Initially, the fine and coarse aggregates were mixed with half of the water for 1 min in the mixer. The rubber was then added to the container and mixed with the aggregate and half of the

water for another 1 min. Subsequently, the binders (cement, fly ash and silica fume) and the superplasticiser were added in the container with the remaining half of the water and mixed for more than 3 mins. The mixtures were then placed in steel forms and compacted using a vibrating table until the air content in the fresh mix was at a minimum. Shorter vibration time was chosen for mixes with higher rubber content to avoid potential floating of rubber particles.

Cylindrical samples of size Ø75 mm × 150 mm were prepared for testing in accordance with EN 12390-1 [67] provisions. After pouring the concrete in the steel forms, they were covered with plastic sheets for 48 hours before de-moulding. The samples were cured in the curing room for up to 28 days. Prior to testing, the loading surfaces of all the cylinders were ground to ensure full contact between the loading device and the samples. All the samples were oven dried for 24 hours in an environmental chamber at 105°C until a constant mass was achieved and cooled down for another 12 hours at ambient temperature prior to testing. The longitudinal dimension and diameter of each sample were measured at three different locations to obtain the average values to assess the σ-ε characteristics as a function of the load-displacement (P-δ) recorded in the tests.

2.2 Testing arrangement

The cylindrical specimens were tested in a stiff Instron Satec 3500 kN machine. All the tests were conducted in displacement control with three levels of compressive cyclic displacement rates of: 0.25 mm/min, 25 mm/min and 250 mm/min, corresponding to strain rates of $\acute{\varepsilon}_1=1.67\times10^{-5}$, $\acute{\varepsilon}_2=1.67\times10^{-3}$ and $\acute{\varepsilon}_3=1.67\times10^{-2}$ sec^{-1}, respectively. As shown in Figure 2a, the test specimens were located on a high-strength steel loading plate with a diameter of 75 mm and thickness of 60 mm, whereas a 3D hinge with a total thickness of 100mm was placed at the top of the specimen. The bottom loading plate was a stiff 100 mm thick steel element to avoid direct contact between the displacement measurement ring system and the test machine. An intermediate plate was placed between the specimen and the test machine, hence allowing measurement of the total compressive deformation of the specimen in the post-peak regime.

The pre-peak axial compressive behaviour of the cylindrical specimen was recorded through three displacement transducers positioned symmetrically around the specimen, and were fixed on two steel rings at a gauge length of 95 mm (Figure 2b). This measuring technique provides reliable measures measurement of axial deformations of the cylindrical specimen along the gauge length, without the influence of test set-ups such as the stiffness of the test rig as well as the gaps between loading plates [68]. Each ring was attached to the surface of the sample through three steel bolts in order to avoid direct contact with the specimen. Two additional transducers were placed between

the bottom of the test machine and the intermediate plate on the top of the specimen to measure the post-peak deformation as, due to severe cracking, ring transducer recordings would become unreliable [68]. The two independent measurement systems were required in order to assess the complete σ-ε characteristics, as the pre-peak deformations were stable whilst the post-peak regimes were governed by unstable crack propagations. The recorded displacements from the transducers were averaged and converted to strains by the gauge length of each measurement setting. The specimen ends were provided with jubilee clips to achieve reliable failure modes under compression.

Both monotonic and cyclic loading scenarios were carried out in this study for all three loading rates. For the monotonic loading cases, incremental displacements were applied to the specimens until they reached failure. For the cyclic loading cases, a pre-loading of approximately 30% of the monotonic compressive strength was applied in order to stabilise the system and minimise the gaps between the tested specimen and loading plates. The sequence applied in the cyclic loading cases is shown in Figure 3. Three cycles of loading/unloading were applied at each displacement level. In the pre-peak region, a displacement increment of 0.1 mm was considered in each step until the specimen reached the crushing region. After crushing, the displacement increment was increased gradually up to failure.

3 Stress-strain behaviour

As noted above, material characterisation tests on conventional (CCM) and rubberised concrete (RuC) cylinders were carried out to assess the influence of rubber content and loading rates on the monotonic and cyclic compressive behaviour. The volumetric rubber replacement ratios were 0, 10%, 20%, 30% and 40% (i.e. ρ_{rv}=0, 0.1, 0.2, 0.3, 0.4) of the total aggregates as described in the previous section. Figure 4 depicts the typical stress-strain (σ-ε) response of all specimens assessed as the average of 3 tests in each case. The monotonic test results are also presented separately in Figure 5(a)-(c). Detailed mechanical properties of the tested specimens, corresponding to each ρ_{rv} and loading rate, are given in Table 3. The average monotonic σ-ε of each set of tests is provided along with the average cyclic characteristics. The specimen reference adopts the format Rxx-Sy-C/M which indicates the volumetric rubber content (R) in percentage, the loading rate (S1=0.25mm/min, S2=25mm/min, and S3=250mm/min, corresponding to $\acute{\varepsilon}_1$, $\acute{\varepsilon}_2$, and $\acute{\varepsilon}_3$, respectively) and the loading type (C: cyclic loading; M: monotonic loading). Characteristic failure patterns of selected CCM and RuC specimens are also shown within Figure 4.

3.1 Monotonic response

The response of an unconfined concrete sample under compression can be represented by three main regions as shown in the schematic envelope of concrete materials under compression in Figure 6. An elastic regime up to about 30% of the compressive strength, followed by a hardening regime characterised by a non-linear response and stiffness softening around the peak due to micro-cracking. For RuC materials (R10-R40), after the crushing strain is reached, the behaviour is characterised by macro-cracking and damage accumulation, represented by softening which is affected by the concrete strength. Relatively high strength concrete (R00) tends to have a brittle response with low ductility and a steep descending branch, whilst those with relatively lower strength are typically more ductile. Tests carried out previously by the authors on RuC [9] showed that a softer post-crushing behaviour occurs with increasing rubber content, typically leading to increased material ductility.

The stress-strain (σ-ε) curves shown in Figure 5(a)-(c) and the results given in Table 3 show that the increase in rubber content (ρ_{rv}) caused reduction in the compressive strength (f_{rc}), elastic modulus (E_{rc}) and crushing strain ($\varepsilon_{rc,0}$). These are in accordance with observations from previous studies by the authors in which the rubber blend included particles up to 20 mm, even though in this study rubber particles up to 2.5 mm only were used [9]. The compressive strength f_{rc} of RuC with ρ_{rv}=0.4 (R40) was about 20% of the reference CCM (R00). E_{rc} was also reduced to about 40% when ρ_{rv} varied from 0 to 0.4. On the other hand, the post-peak behaviour showed increased softening with the increase in ρ_{rv}. As shown in Figures 4 and 5, the brittle failure mode of the reference CCM (R00) exhibited no post-peak deformation whereas the RuC specimens developed a relatively softer post-peak behaviour, typically characterised by high energy dissipation in the post-crushing regime.

For specimens subjected to the static loading rate (S1), as the rubber replacement ratio reached ρ_{rv}=0.4, the compressive strength f_{rc} was about 22% of the reference concrete. E_{rc} of RuC with 40% of rubber also reduced to 40% of the elastic modulus (E_{c0}) of the reference concrete. Meanwhile, the crushing strain $\varepsilon_{rc,0}$ of R40 had a reduction of 40% compared to that of R00. The average $f_{rc,R00\text{-}S1\text{-}M}$=82.6MPa, $E_{rc,R00\text{-}S1\text{-}M}$=40.0GPa and $\varepsilon_{rc,0,R00\text{-}S1\text{-}M}$=0.216% were obtained for normal concrete specimens under the static loading rate. For the RuC specimens under the S1 rate, the recorded average f_{rc} were 58.1 MPa, 36.2 MPa, 25.9 MPa and 17.8 MPa for R10, R20, R30 and R40 specimens, respectively. Meanwhile, the average E_{rc} and $\varepsilon_{rc,0}$ were 30.5 GPa and 0.19% for ρ_{rv}=0.1, 25.9 GPa and 0.14% for ρ_{rv}=0.2, 21.5 GPa and 0.132% for ρ_{rv}=0.3, and 15.7GPa and 0.13% for ρ_{rv}=0.4. As shown in Figure 5(d)-(f), the comparison between the monotonic test results in this

study and the RuC properties obtained from a previous study indicated largely the same influence of ρ_{rv} on the properties of RuC [9]. The compressive strength (f_{rc}), elastic modulus (E_{rc}) and crushing strain ($\varepsilon_{rc,0}$) of RuC in the figure are normalised with respect to the corresponding values for CCM (f_{c0}, E_{c0} and $\varepsilon_{c0,0}$), respectively.

Figure 5 and Table 3 also compare the static S1 ($\acute{\varepsilon}_1$) and higher-rate S2 and S3 ($\acute{\varepsilon}_2$ and $\acute{\varepsilon}_3$) mechanical properties of RuC specimens obtained from the monotonic σ-ε curves. It is shown that the increase in strain-rate ($\acute{\varepsilon}$) increases f_{rc}, E_{rc} and $\varepsilon_{rc,0}$ for RuC, with the enhancement ratio being largely constant with the increase in ρ_{rv}. The increase in $\acute{\varepsilon}$ results in an increase in the compressive strength f_{rc} of RuC for all ρ_{rv} by an average of 12.1% (for $\acute{\varepsilon}_2$) and 18.3% (for $\acute{\varepsilon}_3$), respectively (Figure 5(d)). The corresponding increase in crushing strain $\varepsilon_{rc,0}$ is 6.0% and 11.7%, respectively (Figure 5(f)). It is noted from Figure 5(b) that the increase in $\acute{\varepsilon}$ has a greater influence on R00, R10 and R20 specimens whereas the effect is reduced as the rubber content reaches ρ_{rv}=0.3-0.4. Unlike the compressive strength of RuC, which, among other factors, is controlled by the soft aggregate behaviour of rubber particles and by their interaction with the matrix, the elastic deformability (elastic modulus) of the RuC material is highly influenced by the elastic behaviour of rubber. Studies have shown that although rubber is a rate-sensitive material similar to cementitious composites, the rates applied in this study (between 10^{-5} to 10^{-2} sec^{-1}) have a negligible effect on the constitutive response of rubber [46,47]. Hence, the enhancement in E_{rc} due to the increase in $\acute{\varepsilon}$ is reduced for specimens with high ρ_{rv} ratios.

3.2 Cyclic response

The stress-strain (σ-ε) response of CCM and RuC specimens for different strain rates ($\acute{\varepsilon}$: S1, S2, S3) are shown in Figure 4. The rubber content (ρ_{rv}) influences the cyclic mechanical properties of RuC in a similar manner to those tested under monotonic loading. The cyclic compressive strength (f_{rc}) of R40 is 23% of its reference concrete (R00), combined with a reduction of 33% in both the elastic modulus (E_{rc}) and crushing strain ($\varepsilon_{rc,0}$). The cyclic compressive strength (f_{rc}) of all CCM and RuC specimens loaded under S1 show an average reduction in f_{rc} of 1.3% compared to their monotonic counterparts ($f_{rc,R00\text{-}S1\text{-}C}$=79.0MPa, $f_{rc,R10\text{-}S1\text{-}C}$=55.5MPa, $f_{rc,R20\text{-}S1\text{-}C}$=36.3MPa, $f_{rc,R30\text{-}S1\text{-}C}$=25.8MPa and $f_{rc,R40\text{-}S1\text{-}C}$=18.4MPa). E_{rc} shows average reductions of 4.4%, whilst the average cyclic crushing strain is unchanged compared to the monotonic cases. E_{rc} and $\varepsilon_{rc,0}$ were 39.1 GPa and 0.204% for CCM, 30.6 GPa and 0.190% for R10, 26.2 GPa and 0.147% for R20, 20.6 GPa and 0.136% for R30, and 13.1 GPa and 0.138% for R40.

The cyclic and monotonic mechanical characteristics for all specimens with different ρ_{rv} and subjected to the three loading rates are presented in Figure 7. As observed from Figure 7(a)-(c), the highest f_{rc} and E_{rc} are obtained for specimens tested under the monotonic rate S3, whilst the lowest bounds are those tested under cyclic rate S1. The average cyclic-to-monotonic reduction ratios in strength and stiffness of RuC materials for all strain rates are 3.6% and 6.4%. The change in $\acute{\varepsilon}$ shows almost no effect on the cyclic-to-monotonic $\varepsilon_{rc,0}$ ratios for all RuC materials. The experimental observations indicate that ρ_{rv} has a similar influence on both cyclic and monotonic mechanical properties of RuC, whereas specimens loaded under higher $\acute{\varepsilon}$ develop enhanced f_{rc} and E_{rc}. Meanwhile, cyclic loading has a relatively insignificant influence on f_{rc} and E_{rc} for both CCM and RuC compared to monotonic loading conditions.

Similarly to the monotonic loading cases, Figure 4 indicates that the cyclic σ-ε response of RuC materials with relatively high ρ_{rv} are relatively ductile and develop a stable post-crushing hysteresis. The high strength CCM specimens show brittle failure under cyclic loading without any post-crushing σ-ε branch. Moreover, most of the post-peak energy of R10 and R20 RuC specimens is dissipated within the first cycle after crushing due to the relatively brittle behaviour caused by the formation of a single major crack. On the other hand, the RuC specimens with relatively high rubber content (R30 and R40) demonstrate a much more stable accumulation of hysteretic energy, characterised by the formation of several macro-cracks in the post-peak regime.

To quantify the influence of ρ_{rv}, $\acute{\varepsilon}$ and loading type on the post-crushing response of CCM and RuC, the crushing energy (G_{cl}) was assessed using the principles illustrated in the diagram located at the bottom left of Figure 7(d). G_{cl} was evaluated as the grey area under the σ-ε envelope up to the recorded residual stress of $0.3\times f_{rc}$. This includes the triangular area in the pre-peak regime and the area below the post-peak curve. The parameter $G_{cl,mono}$ (N/mm^2) may be defined as the energy dissipated per unit volume of the specimen during monotonic compressive deformation. The corresponding $G_{cl,cyc}$ for specimens under cyclic loading is referred to as the accumulation of hysteretic energy of the first loading cycle at each applied deformation level down to $0.3\times f_{rc}$.

The influence of ρ_{rv} and $\acute{\varepsilon}$ on $G_{cl,mono}$ and $G_{cl,cyc}$ is depicted in Figure 7(d) and Table 3. It is shown that a similar level of G_{cl} is achieved for both cyclic and monotonic loading with an average $G_{cl,cyc}/G_{cl,mono} = 1.02$. A relatively steep reduction in G_{cl} is observed when ρ_{rv} increases from 0.1 to 0.2, as for this range the compressive behaviour seems to be governed by concrete. Hence, the reduction in G_{cl} is largely proportional to the reduction in f_{rc}. When $\rho_{rv} \geqslant 0.2$, G_{cl} is largely constant

as the reduction in f_{rc} stabilises, and a more ductile post-peak response develops. Beyond ρ_{rv}= 0.2, the rubber governs the material behaviour rather than the concrete.

The material tests described in this section enabled a direct assessment of the effects of rubber content (ρ_{rv}) and strain rate ($\acute{\varepsilon}$) on the monotonic and cyclic mechanical properties of RuC materials. Detailed insights into the strength and stiffness degradation properties as well as post-crushing performance of RuC, were obtained. Other representative material parameters for concrete under cyclic loading are discussed in detail in the following section, including the cumulative energy dissipation, inter-cycle degradation, unloading stiffness and unloading residual strain.

4 Characterisation of cyclic response

In addition to the experimental results presented in Section 3, which focussed on the mechanical characteristics of CCM and RuC materials loaded at different strain rates and conditions, a detailed assessment of the hysteretic behaviour of 36 RuC specimens is presented in this section. The assessment focuses on the cyclic tests on RuC materials with rubber content ρ_{rv}=0.1-0.4 and subjected to the three different strain rates (S1, S2 and S3) as mentioned before (corresponding to $\acute{\varepsilon}_1$=1.67 × 10^{-5}, $\acute{\varepsilon}_2$=1.67 × 10^{-3} and $\acute{\varepsilon}_3$=1.67 × 10^{-2} sec^{-1}). The effect of each parameter on the cyclic response of RuC materials is examined and key observations regarding the hysteretic behaviour are presented. In the subsequent discussion, an ultimate strain threshold of ε_{rcu} = 0.8% is considered, which corresponds to a level where the stress reduces to less than 10% of the corresponding compressive strength (i.e. $\sigma < 0.3 \times f_{rc}$).

4.1 Energy dissipation and inter-cycle stability

The energy dissipation of the unit volume of RuC specimens is estimated from the cyclic σ-ε shown in Figure 4 as the enclosed areas of each cyclic loop in the post-peak regime. The sum of the dissipated energy at each first cyclic loop from crushing to the ultimate strain threshold, referred to as the cumulative dissipated energy E_{DC} (N/mm^2), is presented in Figure 8. This parameter enables the evaluation of rubber content (ρ_{rv}) and strain rate ($\acute{\varepsilon}$) effects on the energy dissipation capacity of RuC materials under static and higher-rate cyclic compressive loads.

Firstly, Figure 8(a)-(d) indicates that RuC materials with less rubber show higher E_{DC} due to the relatively higher compressive strengths. At the ultimate state, the R10 specimen under the static strain rate S1 has $E_{DC, R10\text{-}S1}$ = 0.081 N/mm^2, which is 19%, 27% and 36% higher than its R20, R30 and R40 counterparts, respectively (i.e. $E_{DC, R20\text{-}S1}$ = 0.066 N/mm^2 $E_{DC, R30\text{-}S1}$ = 0.059 N/mm^2 and $E_{DC, R40\text{-}S1}$ = 0.052 N/mm^2). Comparative assessments of the results from Figures 4 and 7 indicate

that, due to the relatively brittle failure modes of R10 and R20 specimens, most of the energy was dissipated within the first loading cycle.

It can also be noted that RuC specimens loaded under the higher strain rates (S2 and S3) show higher E_{DC} compared to those under static loading conditions (S1). It is also shown that for R10 and R20 specimens, the increase in strain rate ($\dot{\varepsilon}$) for S2 and S3 leads to an enhancement of E_{DC} at crushing by 25% and 36%, respectively. In contrast, the influence of $\dot{\varepsilon}$ on E_{DC} at crushing for R30 and R40 is negligible. In general, the increase of $\dot{\varepsilon}$ from S1 to S3 shows constant enhancement of E_{DC} at ultimate state (ε_{rcu} = 0.8%) irrespective of ρ_{rv}, with an average increase of 33.7%.

Figure 9 shows the increase in rate of E_{DC} in relationship with axial strain after crushing, denoted as λ and determined as the ratio between the E_{DC} at a specified strain level and the strain at crushing. It is noted from Figure 9(a)-(c) that the increase in ρ_{rv} results in a significant enhancement in λ at each strain rate level. As described previously, most of the energy for R10 and R20 specimens is dissipated in the first cycle after crushing, whereas less energy is dissipated in the following cycles up to the ultimate state, highlighting the largely brittle post-peak behaviour of these RuC materials. On the other hand, although R30 and R40 specimens dissipated a lower amount energy after crushing, as shown in Figure 4 and 7, the increase in ρ_{rv} allows the material to absorb larger amounts of energy in the subsequent cycles leading to up to 18 times higher λ than those of R10 and R20 specimens. These observations also indicate a more ductile and stable post-peak behaviour for RuC with relatively high ρ_{rv} in comparison to those with lower ρ_{rv}.

Inter-cycle stability is another key property to describe the energy dissipation and degradation response of concrete materials under cyclic loading, and such studies on RuC have been lacking to date. For comparison purposes, an inter-cycle stability factor (υ) is defined as the ratio between the energy dissipated in the third cycle and that dissipated in the first cycle. This is assessed for all RuC specimens in strain level ranges between 0.4% > ε_{rc} > ε_{rcu}, where unstable crushing occurs. Higher values of υ indicate better inter-cycle stability, whilst relatively low values are representative of significant inter-cycle degradation.

It is shown in Figure 10(a)-(c) that the inter-cycle stability of RuC materials increases with ρ_{rv}, with 40% rubber producing an enhancement in υ by up to two folds compared to that of ρ_{rv} = 0.1. Rubber particles have a clear contribution to the recovery of RuC after unloading, leading to a more stable material degradation response. Although υ reduces with the development of axial strain due to the overall degradation of the material, the strain rates ($\dot{\varepsilon}$) have a negligible influence on the inter-cycle stability of RuC materials. The values of υ_{R40} and υ_{R30} (for ρ_{rv} = 0.4 and 0.3, respectively) are

relatively similar, varying in the range of 0.28-0.40 for different ε̇, whilst υ_{R20}=0.33-0.20 (for ρ_{rv} = 0.2) and υ_{R10}=0.22-0.1 (for ρ_{rv} = 0.).

This section has examined the effects of ρ_{rv} and ε̇ on the ductility and stability of RuC materials under cyclic loading in the post-crushing regime. Although RuC with relatively high rubber content dissipated less energy, represented by lower nominal E_{DC} values, the cumulative dissipated energy in the post-crushing regime is more stable than that of RuC with lower rubber contents. These characteristics indicate a more ductile crushing behaviour for high-ρ_{rv} RuC. High strain rates induce additional dissipated energy, yet these have a generally negligible influence on the inter-cycle stability of RuC materials.

4.2 Unloading modulus and residual strain

The unloading path, represented by the unloading modulus (E_{un}) and the corresponding residual strain (ε_{res}), is used to describe the compression recovery of concrete under cyclic loading and to quantify the damage propagation in the material. The envelope schematic of concrete under compression in Figure 6 shows a σ-ε for concrete under cyclic compressive loading. The residual strain ε_{res} is defined as the strain corresponding to a zero or near-zero stress on the unloading σ-ε path whilst the unloading modulus E_{un} is defined as the second modulus of the unloading path. The effects of rubber content (ρ_{rv}) and strain rate (ε̇) on the RuC unloading modulus E_{un} of the first loading cycle at each strain level are depicted in Figure 11. It is evident that the E_{un} of RuC material reduces significantly with the increase in axial strain. As shown in Figure 11(a)-(c), for R10 and R20, E_{un} reduces by 60% and 77% compared to the corresponding elastic modulus (E_{rc}), demonstrating a significant material degradation. On the other hand, R30 and R40 specimens demonstrate a similar E_{un} at crushing, whilst the change in E_{un} with axial strain indicates a gradual material degradation in consecutive cycles. Under unloading, degradation of axial stiffness occurs as the strains increase, and the unloading modulus can generally be represented by a damage index which is proportional to strain softening and degradation [24].

For all the strain rates (ε̇), specimens with higher ρ_{vr} show lower E_{un} due to the inherently low stiffness of RuC material and the elastic recovery ability of rubber particles. Close inspection of Figure 11(a)-(c) shows that the difference between $E_{un,R10}$ (ρ_{vr}=0.1) and $E_{un,R40}$ (ρ_{vr}=0.4) is greater with the increase in ε̇. Similar to the investigation on E_{rc}, described in Section 3.1, the compressive recovery modulus of RuC material with high ρ_{vr} is greatly influenced by the rubber particles which show less sensitivity to the ε̇ range considered in this study. Hence, the increase in strain rate from

10^{-5} to 10^{-2} sec^{-1} provides higher enhancement to the E_{un} of R10 and R20 specimens, whereas the influence of έ on R30 and R40 specimens is comparatively insignificant.

The residual strain (ε_{res}) propagation with the axial strain after crushing of all the tested RuC specimens is shown in Figure 12(a)-(c). It is noted that ε_{res} of RuC reduced significantly as the rubber content increased from ρ_{rv} = 0.1 to ρ_{rv} = 0.4, with an average reduction ratio of 32%. It is shown that the increase in ρ_{rv} has a positive influence on the compression recovery of RuC, whilst the increase in έ has a minimal effect on the accumulation of ε_{res}. On the other hand, the accumulation of ε_{res} for R10 shows a linear relationship with the increase in axial strain ε, whereas ε_{res} of higher rubber contents shows an increased accumulation rate with the propagation of axial strain. The elastic characteristics of rubber particles provide additional effects on the tension recovery after removal of applied compressive load. This effect restricts the propagation of residual deformation in the RuC material in the post-crushing cycles. Further increases in axial strain causes severe debonding between the aggregates and the cement paste, leading to a reduction in the rubber recovery effect and faster accumulation of ε_{res}. An increase in axial strain in the post-peak regime is characterised by a sliding diagonal macro-crack. Under sliding, the crack interfaces are locked by the mineral aggregates (aggregate interlock action) and by rubber particles (rubber clamping action) [10]. As the width and slip of the macro-crack increase, the aggregates and particles debond from one of the crack interfaces, typically on the side with the lowest particle embedment area. Such effects would develop in unconfined RuC cylinders under compression.

The test results shown in Figure 11 and Figure 12 permit the development of assessment expressions for E_{un} and ε_{res} of RuC based on a set of regression analyses. The unloading stiffness characteristics are shown in Figure 13(a) through an 'E_{norm} versus A' relationship as proposed in Equation 1. The parameter E_{norm} in Equation 1 (a) represents the ratio between the unloading stiffness E_{un} and the elastic modulus E_{rc}, whereas the unitless parameter A in Equation 1(b) represents the relationship between the axial strain ε, the crushing strain $\varepsilon_{rc,0}$ and the rubber content ρ_{rv}. By combining Equations 1(a) and 1(b), the unloading stiffness E_{un} can be obtained (Equation 1(c)). As indicated in Figure 13(a), there is a good agreement between the test and predicted results, with an average analysis-to-experiment ratio of 0.99 and a COV of 0.18. It is also worth noting that Equation 1 represents the behaviour of E_{un} of RuC subjected to all the strain rate ranges applied in this study, as the strain rate had limited influence on E_{un}

$$E_{norm} = \frac{E_{un}}{E_{rc}} \tag{1a}$$

$$A = (\frac{\varepsilon}{\varepsilon_{rc,0}} - 1) \times (-3.4\rho_{rv} + 2.4) + 1 \quad (1b)$$

$$E_{un} = \left(0.97A^{-1.9} + 0.03\right) E_{rc} \quad (1c)$$

A set of expressions for the assessment of ε_{res} of RuC as a function of ρ_{rv} and the strain rate is proposed, as both parameters influence the cyclic RuC properties. This is represented by a 'B versus ε_{norm}' relationship, shown in Figure 13 (b). The parameters B and ε_{norm} in Equation 2 (a)–(c) represent the normalised residual strain and axial strain of the material, respectively. A set of fitting parameters (λ_{S1}, λ_{S2} and λ_{S3}) were introduced to represent the influence of strain rate on ε_{res}. As indicated in Figure 13 (b), the proposed expressions show good agreement with the experimental results of all strain rates, with an average analysis-to-experiment ratio of 0.91 for S1, 0.87 for S2 and 0.84 for S3, with a COV of 0.14, 0.17 and 0.18 respectively. Equations (1-2) can be used in conjunction with existing constitutive models for conventional concrete [18,19,24] in order to obtain the complete cyclic compressive response.

$$B = (\frac{\varepsilon_{res}}{\varepsilon_{res,0}} - 1) \times \lambda + 1 \quad (2a)$$

$$\varepsilon_{norm} = \frac{\varepsilon}{\varepsilon_{rc,0}} \quad (2b)$$

$$B = 3.14\varepsilon_{norm}{}^2 + 7.2\varepsilon_{norm} - 9.3 \quad (2c)$$

$$\text{where} \quad \lambda = \begin{Bmatrix} -400\rho_{rv}{}^3 + 285\rho_{rv}{}^2 - 49.5\rho_{rv} + 3.5 \;\; for \;\; (S1) \\ 60\rho_{rv}{}^3 - 32.5\rho_{rv}{}^2 + 13.05\rho_{rv} - 0.41 \;\; for \;\; (S2) \\ 342\rho_{rv}{}^3 - 211\rho_{rv}{}^2 + 41.9\rho_{rv} - 1.94 \;\; for \;\; (S3) \end{Bmatrix}$$

and $\varepsilon_{res,0}$ - the residual strain on the unloading curve initiated at peak (see Figure 6)

The above observations also indicate that rubber particles have a beneficial effect on the energy dissipation, as they provide less inter-cycle degradation and improved stability in the post-crushing regime.Based on the studies carried out in this paper, it is shown that CCM have a largely brittle response without any post-peak ductility, whilst by addition of a small proportion of rubber (10%) there are significant benefits in terms of post-crushing characteristics. Whilst the properties of RuC with 10% and 20% rubber are largely governed by the concrete matrix, the influence of the constituent rubber becomes more pronounced for 30% and 40% replacement ratios. This was

particularly evident from the assessment of the unloading modulus and residual strains resulting from repeated loading cycles.

Previous experimental and numerical studies on the cyclic behaviour of reinforced rubberised concrete (RRuC) members carried out by the authors indicate that the increase in rubber content has little influence on the performance of flexural members such as beams with no or very low axial loads [16, 59]. The results presented in this study, which has been lacking to date, regarding the fundamental cyclic properties of unconfined RuC materials, show that RuC can be used in expected plastic hinge zones of flexural members. On the other hand, for RRuC members with high axial loads such as column members, external confinement such as using steel tubes or FRP jackets [15, 27, 36, 69, 70], are required. However, for detailed numerical modelling of confined RuC, fundamental characteristics of unconfined RuC under cyclic loading are needed as have been quantified in this paper.

5 Concluding remarks

This paper has examined the effect of rubber content and strain rate on the behaviour of rubberised concrete (RuC) materials under monotonic and cyclic compressive loading. A detailed account of a series of ninety cylindrical specimens with significant rubber content ratios of up to 40%, tested under three different strain rates, representing static, moderate seismic and severe seismic loading, was given. The increase in rubber content was shown to have a detrimental effect on the stiffness and strength, as expected. The results obtained in this investigation, when compared to those from previous studies, also indicate that the rubber particle size has insignificant or no influence on the degradation in mechanical properties. It was also shown that the monotonic compressive strength and crushing strain of RuC were higher by 18.3% and 11.7%, respectively, when the strain rate increased from static loading to that representing severe seismic loading.

The influence of rubber content and strain rate on the mechanical properties and stress-strain response of RuC under cyclic loading was similar to that under monotonic conditions, noting that the cyclic stress-strain envelope was generally contained within the monotonic counterpart. As the rubber content increased from 0 to 20%, the crushing energy showed an initial reduction proportional to the compressive strength whereas further increase in rubber content up to 40% provided enhancement in the energy dissipation. Limited influence was observed from the strain rate on the elastic modulus irrespective of the rubber content, and the elastic moduli under cyclic loading were about 5-10% lower than those under monotonic loading. Although concrete with high rubber content dissipated less cumulative energy during cyclic tests, due to its relatively low

compressive strength, an increase in rubber content enhanced the cumulative rate of hysteretic energy with the increase in axial strain in the post-crushing regime. Moreover, less significant inter-cycle degradation was observed for concrete with high rubber content compared to that with low amounts of rubber.

The unloading stiffness of concrete with low rubber content showed an abrupt reduction, of more than 60% in the first cycle at crushing indicating a largely brittle response. In contrast, specimens with high rubber content developed a more gradual material degradation and, hence, more ductility. In the post-peak regime, specimens with higher rubber content showed lower unloading modulus due to the low stiffness of RuC material and the elastic recovery ability of rubber particles. A higher strain rate provided typically greater enhancement in the unloading modulus of RuC with 10% and 20% rubber content, and had less influence on their counterparts with 30% and 40% rubber. The increase in rubber content enhanced the compression recovery of RuC as the elastic property of rubber particles provided additional effects on the tension recovery after removal of the applied compressive stress.

Overall, with the increase in rubber content, rubberised concrete materials are shown to exhibit improved compressive recovery under cyclic loading, coupled with a higher energy accumulation rate, enhanced inter-cycle stability and lower inter-cycle degradation. It is evident that RuC materials have the ability to maintain their energy dissipation ability under higher number of cycles. It is also shown that the increase in strain rate, from static to severe seismic, leads to a notable increase in the stiffness and strength, with these enhancements becoming less significant with the increase in rubber content. The above listed merits of RuC enable potential application of such materials in expected plastic hinge regions of flexural members where material ductility and inter-cycle stability are essential. In contrast, unconfined RuC with relatively high rubber content would be unusable in structural members with high axial loads and external confinement measures are essential for its application in structures. Based on the results of this investigation, expressions for determining the unloading stiffness and residual strain, as a function of rubber content and strain rate, were proposed within the ranges considered. The suggested relationships enable the practical characterisation of rubberised concrete materials for the purpose of understanding the fundamental cyclic properties of such material, and can be employed in conjunction with widely used cyclic constitutive models.

Acknowledgements

The support of Adria Abruzzo, Hope Construction Materials, Elkem and Sika through the provided materials is gratefully acknowledged.

References

[1] Raffoul, S., Garcia, R., Pilakoutas, K., Guadagnini, M., Medina, N.F., 2016. Optimisation of rubberised concrete with high rubber content: An experimental investigation. Construction and Building Materials 124, 391–404. https://doi.org/10.1016/j.conbuildmat.2016.07.054

[2] Gesoğlu, M. and Güneyisi, E., 2007. Strength development and chloride penetration in rubberized concretes with and without silica fume. Materials and Structures, 40(9), 953-964. https://doi.org/10.1617/s11527-007-9279-0

[3] Güneyisi E. Fresh properties of self-compacting rubberized concrete incorporated with fly ash. Materials and structures. 2010 Oct 1;43(8):1037-48. https://doi.org/10.1617/s11527-009-9564-1

[4] Mohammadi I, Khabbaz H, Vessalas K. Enhancing mechanical performance of rubberised concrete pavements with sodium hydroxide treatment. Materials and Structures. 2016 Mar 1;49(3):813-27. https://doi.org/10.1617/s11527-015-0540-7

[5] Bušić, R., Miličević, I., Šipoš, T. and Strukar, K., 2018. Recycled Rubber as an Aggregate Replacement in Self-Compacting Concrete—Literature Overview. Materials, 11(9), p.1729. https://doi.org/10.3390/ma11091729

[6] He, L., Ma, Y., Liu, Q., Mu, Y., 2016. Surface modification of crumb rubber and its influence on the mechanical properties of rubber-cement concrete. Construction and Building Materials 120, 403–407. https://doi.org/10.1016/j.conbuildmat.2016.05.025

[7] Wang, Z., Hu, H., Hajirasouliha, I., Guadagnini, M. and Pilakoutas, K., 2020. Tensile stress-strain characteristics of rubberised concrete from flexural tests. Construction and Building Materials, 236, p.117591. https://doi.org/10.1016/j.conbuildmat.2019.117591

[8] Jalal, M., Grasley, Z., Nassir, N. and Jalal, H., 2020. Strength and dynamic elasticity modulus of rubberized concrete designed with ANFIS modeling and ultrasonic technique. Construction and Building Materials, 240, p.117920. https://doi.org/10.1016/j.conbuildmat.2019.117920

[9] Bompa, D.V., Elghazouli, A.Y., Xu, B., Stafford, P.J., Ruiz-Teran, A.M., 2017. Experimental assessment and constitutive modelling of rubberised concrete materials. Construction and Building Materials 137, 246–260. https://doi.org/10.1016/j.conbuildmat.2017.01.086

[10] Xu, B., Bompa, D.V., Elghazouli, A.Y., Ruiz-Teran, A.M., Stafford, P.J., 2018. Behaviour of rubberised concrete members in asymmetric shear tests. Construction and Building Materials 159, 361–375. https://doi.org/10.1016/j.conbuildmat.2017.10.091

[11] Su, H., Yang, J., Ling, T.C., Ghataora, G.S., Dirar, S., 2015. Properties of concrete prepared with waste tyre rubber particles of uniform and varying sizes. Journal of Cleaner Production 91, 288–296. https://doi.org/10.1016/j.jclepro.2014.12.022

[12] Strukar, K., Šipoš, T.K., Miličević, I. and Bušić, R., 2019. Potential use of rubber as aggregate in structural reinforced concrete element–A review. Engineering Structures, 188, pp.452-468. https://doi.org/10.1016/j.engstruct.2019.03.031

[13] Bompa, D.V. and Elghazouli, A.Y., 2019. Creep properties of recycled tyre rubber concrete. Construction and Building Materials, 209, pp.126-134. https://doi.org/10.1016/j.conbuildmat.2019.03.127

[14] Son, K.S., Hajirasouliha, I. and Pilakoutas, K., 2011. Strength and deformability of waste tyre rubber-filled reinforced concrete columns. Construction and building materials, 25(1), pp.218-226. https://doi.org/10.1016/j.conbuildmat.2010.06.035

[15] Youssf, O., ElGawady, M.A. and Mills, J.E., 2015, August. Experimental investigation of crumb rubber concrete columns under seismic loading. In Structures (Vol. 3, pp. 13-27). Elsevier. https://doi.org/10.1016/j.istruc.2015.02.005

[16] Elghazouli, A.Y., Bompa, D.V., Xu, B., Ruiz□Teran, A.M., Stafford, P.J., 2018. Performance of rubberised reinforced concrete members under cyclic loading. Engineering Structures 166, 526–545. https://doi.org/10.1016/j.engstruct.2018.03.090

[17] Hernández, E., Palermo, A., Granello, G., Chiaro, G. and Banasiak, L.J., 2020. Eco-rubber Seismic-Isolation Foundation Systems: A Sustainable Solution for the New Zealand Context. Structural Engineering International, pp.1-9. https://doi.org/10.1080/10168664.2019.1702487

[18] Bahn, B.Y. and Hsu, C.T.T., 1998. Stress-strain behavior of concrete under cyclic loading. ACI Materials Journal, 95, pp.178-193.

[19] Sima, J.F., Roca, P. and Molins, C., 2008. Cyclic constitutive model for concrete. Engineering structures, 30(3), pp.695-706. https://doi.org/10.1016/j.engstruct.2007.05.005

[20] Vecchio, F.J., 1999. Towards cyclic load modeling of reinforced concrete. ACI Structural Journal, 96, pp.193-202.

[21] Yankelevsky, D.Z. and Reinhardt, H.W., 1989. Uniaxial behavior of concrete in cyclic tension. Journal of Structural Engineering, 115(1), pp.166-182. https://doi.org/10.1061/(ASCE)0733-9445(1989)115:1(166)

[22] Breccolotti, M., Bonfigli, M.F., D'Alessandro, A. and Materazzi, A.L., 2015. Constitutive modeling of plain concrete subjected to cyclic uniaxial compressive loading. Construction and Building materials, 94, pp.172-180. https://doi.org/10.1016/j.conbuildmat.2015.06.067

[23] Sinha, B.P., Gerstle, K.H. and Tulin, L.G., 1964, February. Stress-strain relations for concrete under cyclic loading. In Journal Proceedings (Vol. 61, No. 2, pp. 195-212).

[24] Osorio, E., Bairán, J.M. and Marí, A.R., 2013. Lateral behavior of concrete under uniaxial compressive cyclic loading. Materials and structures, 46(5), pp.709-724. https://doi.org/10.1617/s11527-012-9928-9

[25] Karsan, I.D. and Jirsa, J.O., 1969. Behavior of concrete under compressive loadings. Journal of the Structural Division.

[26] Moustafa, A. and ElGawady, M.A., 2015. Mechanical properties of high strength concrete with scrap tire rubber. Construction and Building Materials, 93, pp.249-256. https://doi.org/10.1016/j.conbuildmat.2015.05.115

[27] Moustafa, A. and ElGawady, M.A., 2016. Strain rate effect on properties of rubberized concrete confined with glass fiber–reinforced polymers. Journal of Composites for Construction, 20(5), p.04016014. https://doi.org/10.1061/(ASCE)CC.1943-5614.0000658

[28] Gholampour, A., Fallah Pour, A., Hassanli, R. and Ozbakkaloglu, T., 2019. Behavior of Actively Confined Rubberized Concrete under Cyclic Axial Compression. Journal of Structural Engineering, 145(11), p.04019131. https://doi.org/10.1061/(ASCE)ST.1943-541X.0002434

[29] Huang, X. and Chen, Y., 2019. Effect of High-Stress Equal Amplitude Cyclic Loading on Mechanical and Deformation Characteristics of Rubber Concrete. Journal of Architectural Research and Development, 3(5). https://doi.org/10.26689/jard.v3i5.877

[30] Gheni, A., Elgawady. M. and Myers, J. 2017. Mechanical characterization of concrete masonry units manufactured with crumb rubber aggregate. ACI Materials Journal, 114(1). https://doi.org/110.14359/51689482

[31] Eldin, N.N. and Senouci, A.B., 1993. Rubber-tyre particles as concrete aggregate. ASCE Journal of Materials of Civil Engineering. 5(4), pp. 478-496. https://doi.org/10.1061/(ASCE)0899-1561(1993)5:4(478)

[32] Alsaif, A., Garcia, R., Figueiredo, F.P., Neocleous, K., Christofe, A., Guadagnini, M. and Pilakoutas, K., 2019. Fatigue performance of flexible steel fibre reinforced rubberised concrete pavements. Engineering Structures, 193, pp.170-183. https://doi.org/10.1016/j.engstruct.2019.05.040

[33] Toutanji, H.A., 1996. The use of rubber tyre particles in concrete to replace mineral aggregates. Cement and Concrete Composites. 18(2), pp 135-139. https://doi.org/10.1016/0958-9465(95)00010-0

[34] Xue, J. and Shinozuka, M., 2013. Rubberised concrete: a green structural material with enhanced energy-dissipation capacity. Construction and Building Materials. 42, pp. 196-204. https://doi.org/10.1016/j.conbuildmat.2013.01.005

[35] Taha, M.M.R., El-Dieb, A.S., Ab El-Wahab, M.A. and Abdel-Hameed, M.E., 2008. Mechanical, fracture, and microstructural investigations of rubber concrete. ASCE Journal of Materials in Civil Engineering. 20(10), pp.640-649. https://doi.org/10.1061/(ASCE)0899-1561(2008)20:10(640)

[36] Raffoul, S., Escolano-Margarit, D., Garcia, R., Guadagnini, M. and Pilakoutas, K., 2019. Constitutive Model for Rubberized Concrete Passively Confined with FRP Laminates. Journal of Composites for Construction, 23(6), p.04019044. https://doi.org/10.1061/(ASCE)CC.1943-5614.0000972

[37] Gholampour, A., Ozbakkaloglu, T. and Hassanli, R., 2017. Behavior of rubberized concrete under active confinement. Construction and Building Materials, 138, pp.372-382. https://doi.org/10.1016/j.conbuildmat.2017.01.105

[38] Grassl, P. and Rempling, R., 2008. A damage-plasticity interface approach to the meso-scale modelling of concrete subjected to cyclic compressive loading. Engineering Fracture Mechanics, 75(16), pp.4804-4818. https://doi.org/10.1016/j.engfracmech.2008.06.005

[39] Chen, X., Bu, J. and Xu, L., 2016. Effect of strain rate on post-peak cyclic behavior of concrete in direct tension. Construction and Building Materials, 124, pp.746-754. https://doi.org/10.1016/j.conbuildmat.2016.08.012

[40] Ross, C.A., Tedesco, J.W. and Kuennen, S.T., 1995. Effects of strain rate on concrete strength. Materials Journal, 92(1), pp.37-47.

[41] Eibl, J. and Schmidt-Hurtienne, B., 1999. Strain-rate-sensitive constitutive law for concrete. Journal of Engineering Mechanics, 125(12), pp.1411-1420. https://doi.org/10.1061/(ASCE)0733-9399(1999)125:12(1411)

[42] Bischoff, P.H., Bachmann, H. and Eibl, J., 1991. Microcrack development during high strain rate loading of concrete. In European conference on structural dynamics Eurodyn'90 (pp. 59-66).
[43] Bischoff, P.H. and Perry, S.H., 1991. Compressive behaviour of concrete at high strain rates. Materials and structures, 24(6), pp.425-450. https://doi.org/10.1007/BF02472016
[44] Li, M. and Li, H., 2012. Effects of strain rate on reinforced concrete structure under seismic loading. Advances in Structural Engineering, 15(3), pp.461-475. https://doi.org/10.1260/1369-4332.15.3.461
[45] Roland, C.M., 2006. Mechanical behavior of rubber at high strain rates. Rubber Chemistry and Technology, 79(3), pp.429-459. https://doi.org/10.5254/1.3547945
[46] Shergold, O.A., Fleck, N.A. and Radford, D., 2006. The uniaxial stress versus strain response of pig skin and silicone rubber at low and high strain rates. International Journal of Impact Engineering, 32(9), pp.1384-1402. https://doi.org/10.1016/j.ijimpeng.2004.11.010
[47] Gray G.T., Blumenthal W.R. Trujillo C. and Carpenter II R.W. 1997. Influence of temperature and strain rate on the mechanical behaviour if Adiprene L-100. Journal de Physique IV, 07(C3). http://dx.doi.org/10.1051/jp4:1997390.07.10.2172/532527
[48] Topçu, I.B. and Avcular, N., 1997. Collision behaviours of rubberized concrete. Cement and Concrete Research, 27(12), pp.1893-1898. https://doi.org/10.1016/S0008-8846(97)00204-4
[49] Najim, K.B. and Hall, M.R., 2012. Mechanical and dynamic properties of self-compacting crumb rubber modified concrete. Construction and building materials, 27(1), pp.521-530. https://doi.org/10.1016/j.conbuildmat.2011.07.013
[50] Ismail, M.K. and Hassan, A.A., 2016. Impact Resistance and Acoustic Absorption Capacity of Self-Consolidating Rubberized Concrete. ACI Materials Journal, 113(6).
[51] Xue, J. and Shinozuka, M., 2013. Rubberized concrete: A green structural material with enhanced energy-dissipation capability. Construction and Building Materials, 42, pp.196-204. https://doi.org/10.1016/j.conbuildmat.2013.01.005
[52] Atahan, A.O. and Yücel, A.Ö., 2012. Crumb rubber in concrete: static and dynamic evaluation. Construction and Building Materials, 36, pp.617-622.https://doi.org/10.1016/j.conbuildmat.2012.04.068
[53] Atahan, A.O. and Sevim, U.K., 2008. Testing and comparison of concrete barriers containing shredded waste tire chips. Materials Letters, 62(21-22), pp.3754-3757. https://doi.org/10.1016/j.matlet.2008.04.068
[54] Zheng, L., Huo, X.S. and Yuan, Y., 2008. Experimental investigation on dynamic properties of rubberized concrete. Construction and building materials, 22(5), pp.939-947. https://doi.org/10.1016/j.conbuildmat.2007.03.005
[55] Liu, F., Meng, L.Y., Chen, G.X. and Li, L.J., 2015. Dynamic mechanical behaviour of recycled crumb rubber concrete materials subjected to repeated impact. Materials Research Innovations, 19(sup8), pp.S8-496. https://doi.org/10.1179/1432891715Z.0000000001733
[56] Feng, W., Liu, F., Yang, F., Li, L. and Jing, L., 2018. Experimental study on dynamic split tensile properties of rubber concrete. Construction and Building Materials, 165, pp.675-687. https://doi.org/10.1016/j.conbuildmat.2018.01.073
[57] Pham, T.M., Chen, W., Khan, A.M., Hao, H., Elchalakani, M. and Tran, T.M., 2020. Dynamic compressive properties of lightweight rubberized concrete. Construction and Building Materials, 238, p.117705. https://doi.org/10.1016/j.conbuildmat.2019.117705
[58] Bischoff, P.H., 1988. Compressive response of concrete to hard impact. PhD thesis, Imperial College of Science and Technology, London.
[59] Xu, B., Bompa, D.V., Elghazouli, A.Y., Ruiz-Teran, A.M. and Stafford, P.J., 2020. Numerical assessment of reinforced concrete members incorporating recycled rubber materials. Engineering Structures, 204(1). https://doi.org/10.1016/j.engstruct.2019.110017
[60] TARMAC, Tarmac Trupak building aggregates, http://www.tarmac.com/building-aggregates/ [Accessed 25 February 2019]
[61] CONICA, Recycled Rubber from Used Tyres, http://www.conica.com/en/commodities/black-granules/rubbergranules/recycled-tyre-rubber/ [Accessed 2 December 2017].
[62] CEN (European Committee for Standardization) EN 933-1:2012 Tests for geometrical properties of aggregates – Part 1: Determination of particle size distribution – Sieving method. CEN, Brussels (Belgium); 2012
[63] CEN (European Committee for Standardization) EN 450-1:2012 Fly ash for concrete – Part 1. Definition, specifications and conformity criteria, CEN, Brussels (Belgium); 2012

[64] ELKEM, Elkem Microsilica Grade 940 for Concrete, https://www.elkem.com/globalassets/silicon-materials/construction/con-940-pds-october-2017.pdf [Accessed 25 February 2019]
[65] Breedon Cement Limited, High Strength 52.5N Cement, https://www.breedongroup.com/images/uploads/products/Portland_Plus_Cement_DS.pdf [Accessed 25 February 2019]
[66] Sika ViscoFlow 2000, High range water reducing/superplasticing concrete admixture with enhanced workability retention, Data sheet, https://sikaconcrete.co.uk/wp-content/uploads/2017/06/Sika-ViscoFlow-2000-PDS.pdf [Accessed 25 February 2019]
[67] CEN (European Committee for Standardization) EN 12390-1:2012 Testing hardened concrete: part 1: Shape dimensions and other requirements for specimens and moulds, CEN, Brussels (Belgium); 2012
[68] Van Mier, J.G.M., Shah, S.P., Arnaud, M., Balayssac, J.P., Bascoul, A., Choi, S., Dasenbrock, D., Ferrara, G., French, C., Gobbi, M.E. and Karihaloo, B.L., 1997. Strain-softening of concrete in uniaxial compression. Materials and Structures, 30(4), pp.195-209. https://doi.org/10.1007/BF02486177
[69] Bompa, D.V. and Elghazouli, A.Y., 2019. Behaviour of confined rubberised concrete members under combined loading conditions. Magazine of Concrete Research, pp.1-19. https://doi.org/10.1680/jmacr.19.00121
[70] Duarte, A.P.C., Silva, B.A., Silvestre, N., De Brito, J., Júlio, E. and Castro, J.M., 2016. Experimental study on short rubberized concrete-filled steel tubes under cyclic loading. Composite Structures, 136, pp.394-404. https://doi.org/10.1016/j.compstruct.2015.10.015

Figures

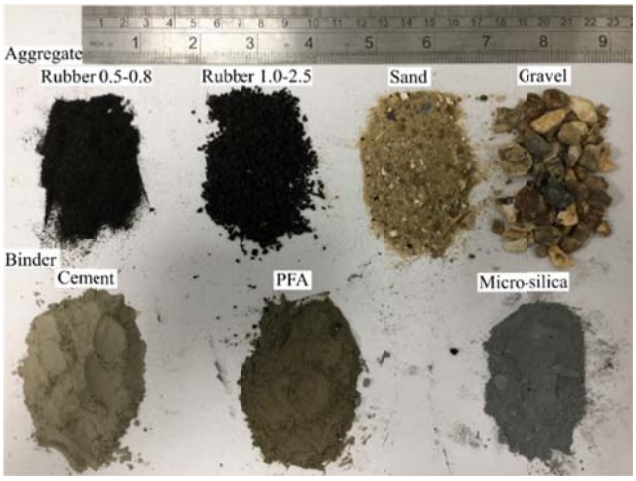

Figure 1 Rubberised concrete constituents

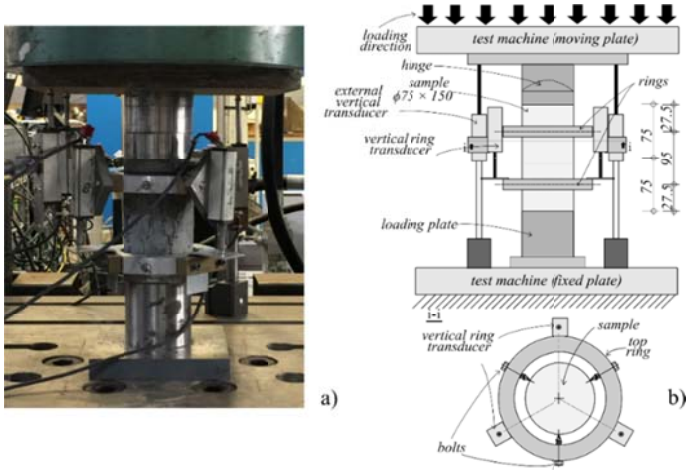

Figure 2 Test arrangement: a) general view, b) layout

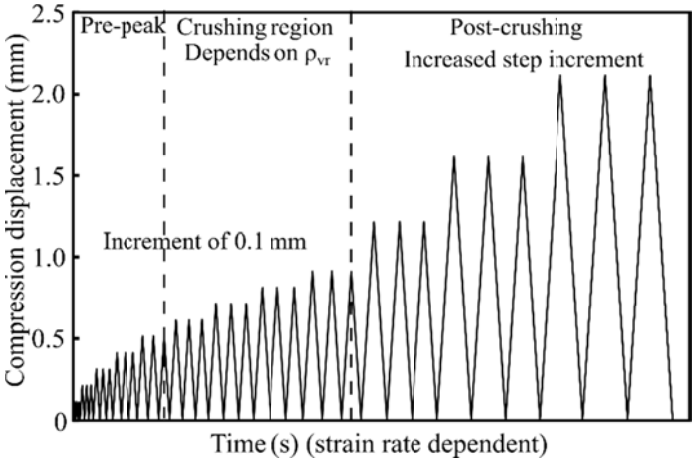

Figure 3 Cyclic loading sequence

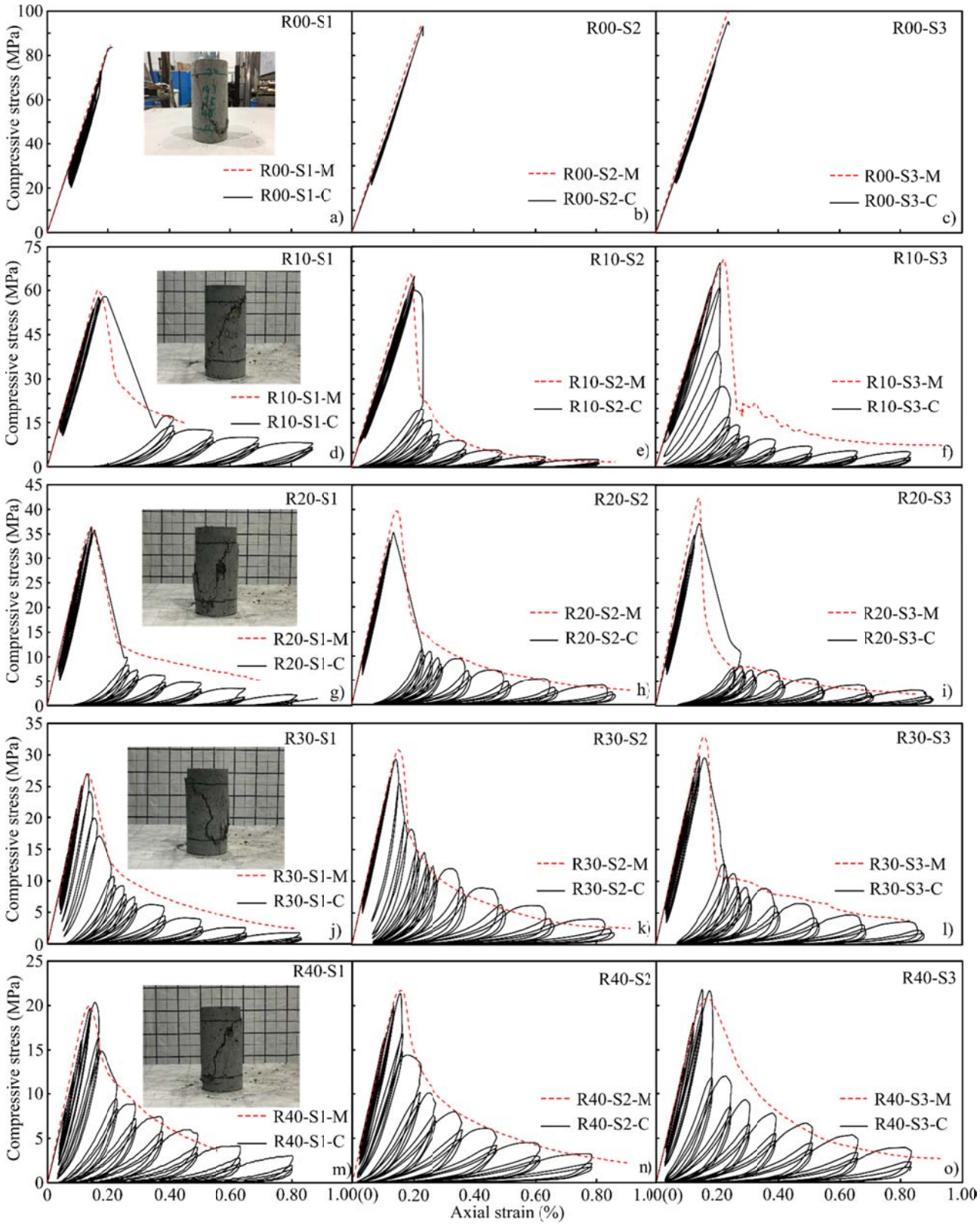

Figure 4 Cyclic stress-strain response of all tested specimens with the monotonic envelopes

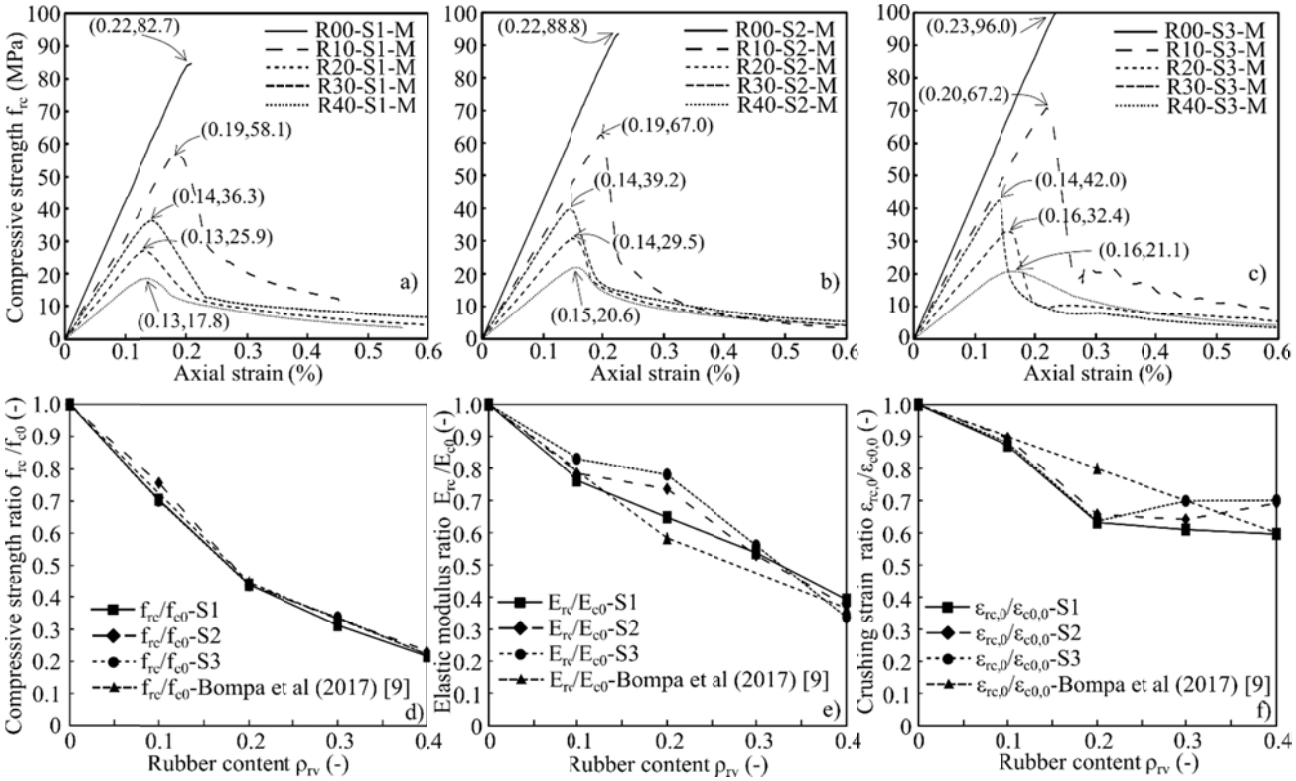

Figure 5 Influence of rubber content and strain rate on the monotonic mechanical properties of RuC: a) compressive strength f_{rc}, b) elastic modulus E_{rc}, c) crushing strain $\varepsilon_{rc,0}$; and comparisons between the results from this paper and previous study by the authors: d) normalised compressive strength f_{rc}/f_{c0}, e) normalised elastic modulus E_{rc}/E_{c0}, f) normalised crushing strain $\varepsilon_{rc,0}/\varepsilon_{c0,0}$

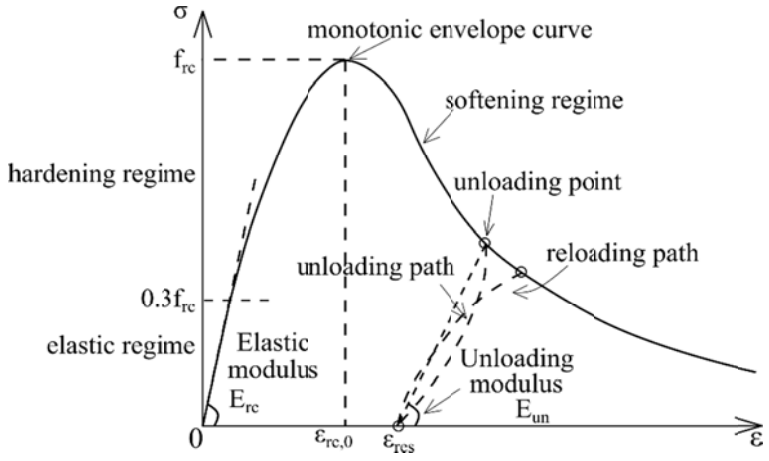

Figure 6 Schematic of concrete materials under cyclic compression

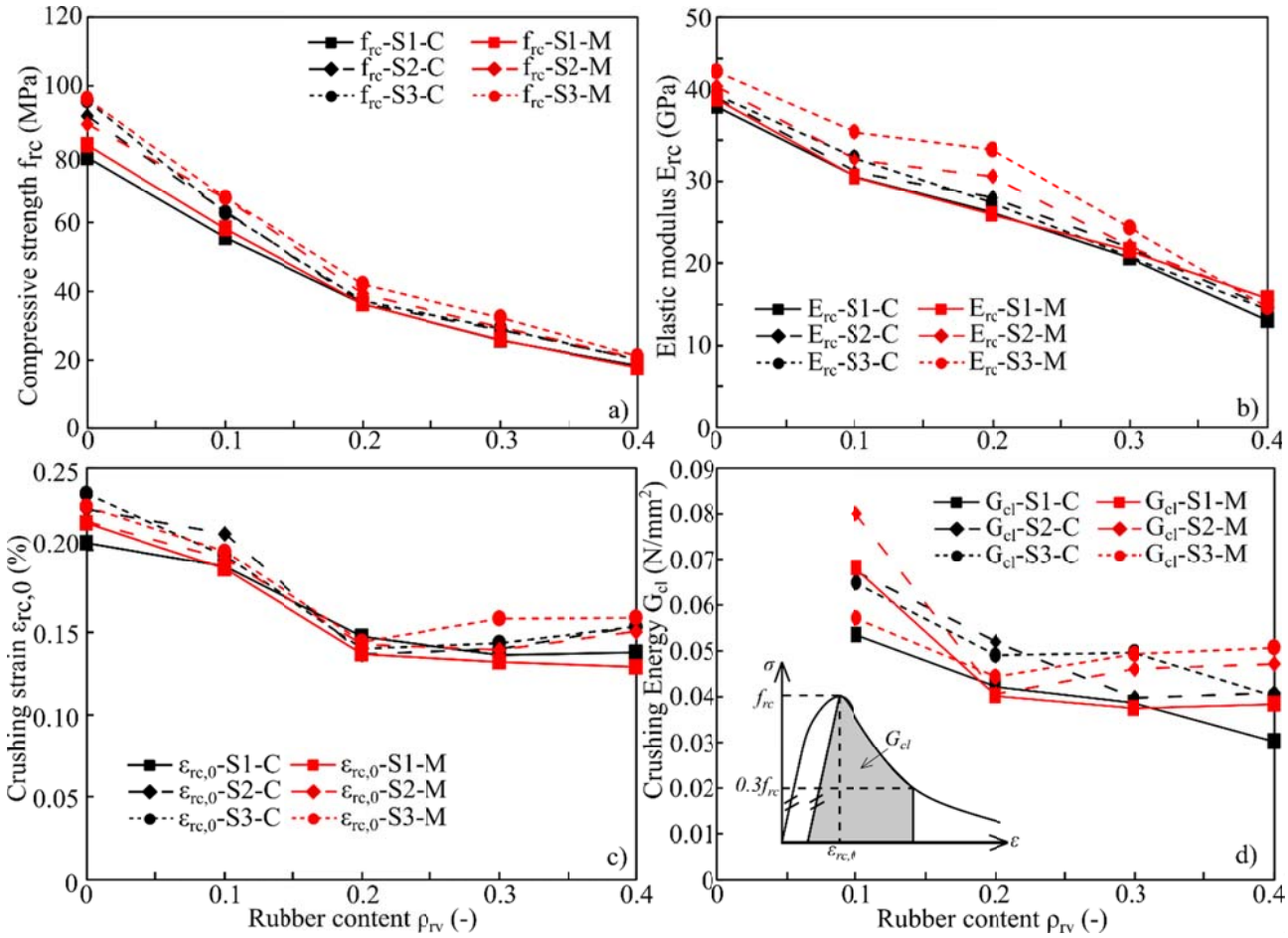

Figure 7 Comparisons of the cyclic and monotonic mechanical properties of RuC: a) compressive strength f_{rc}, b) elastic modulus E_{rc}, c) crushing strain $\varepsilon_{rc,0}$, d) crushing energy G_{cl}

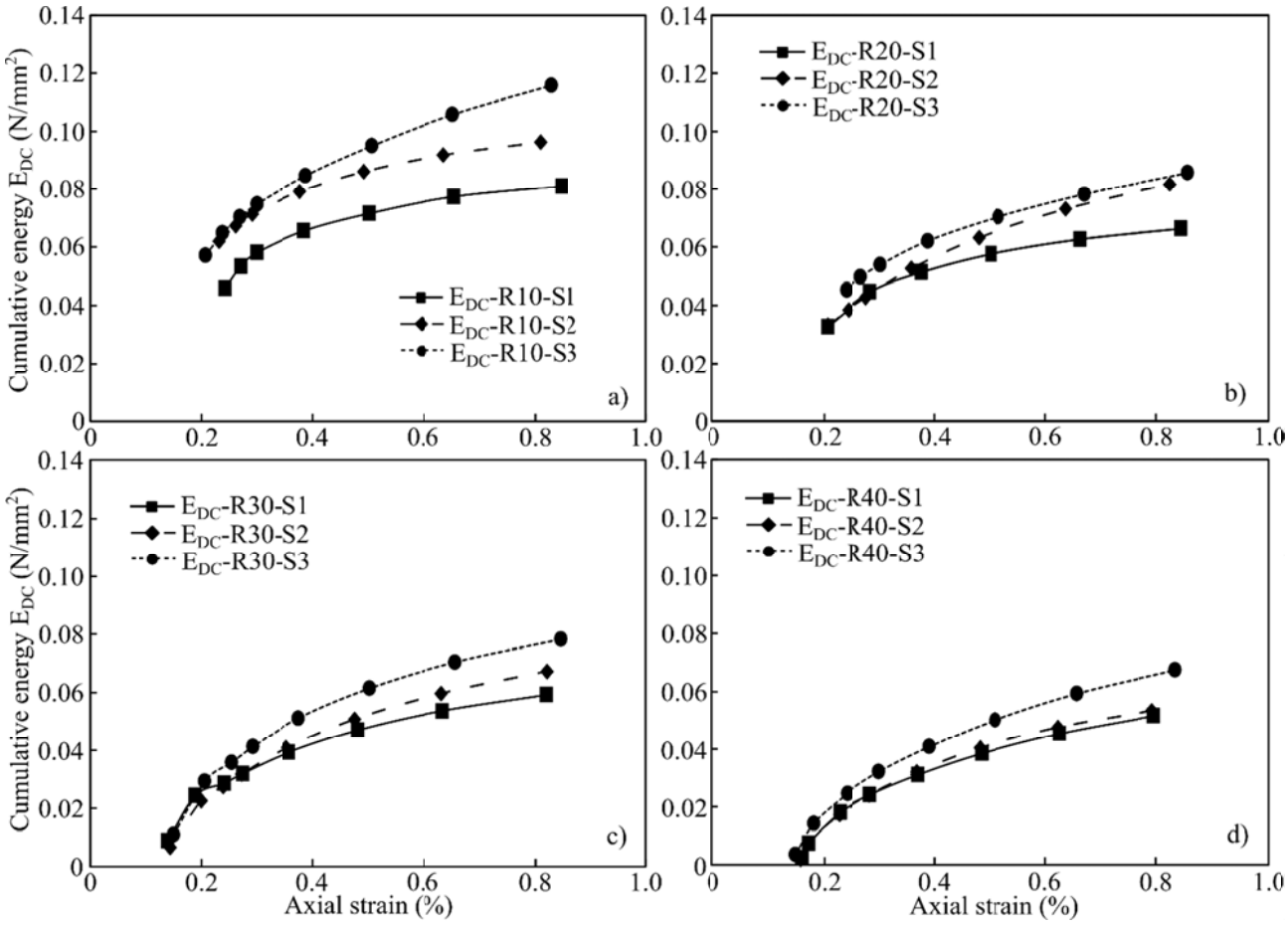

Figure 8 Effect of rubber content and strain rate on the cumulative dissipated energy E_{DC} of the first cyclic loop from crushing strain to target strain level: a) R10, b) R20. c) R30, d) R40 specimens

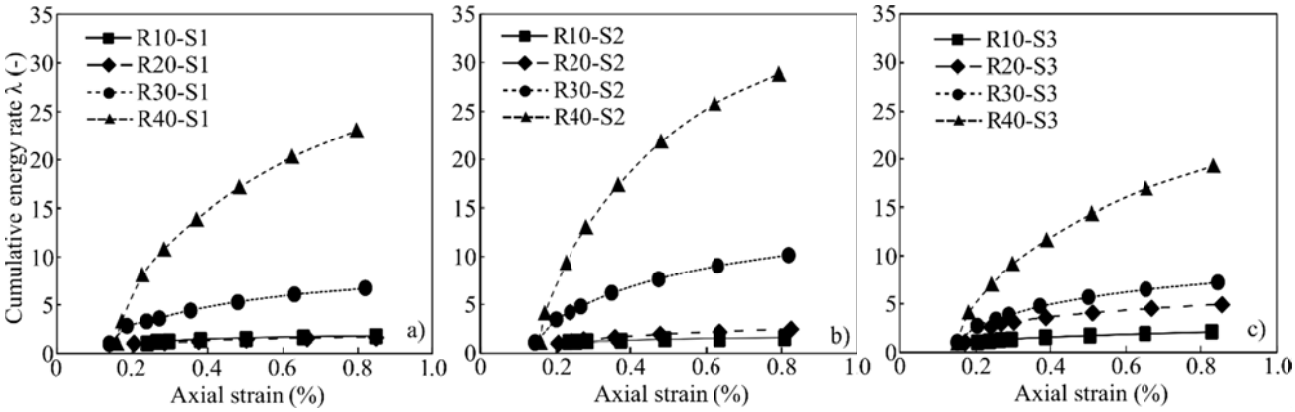

Figure 9 Cumulative energy rate λ of specimens loaded under different strain rates: a) S1, b) S2, c) S3

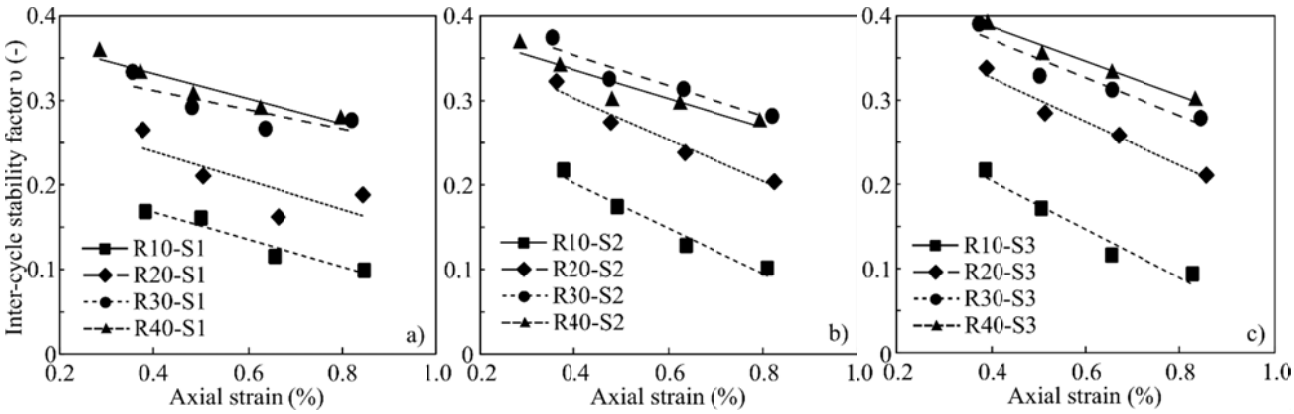

Figure 10 Effect of rubber content on the inter-cycle stability factor υ of RuC specimens loaded under different strain rates: a) S1, b) S2, c) S3

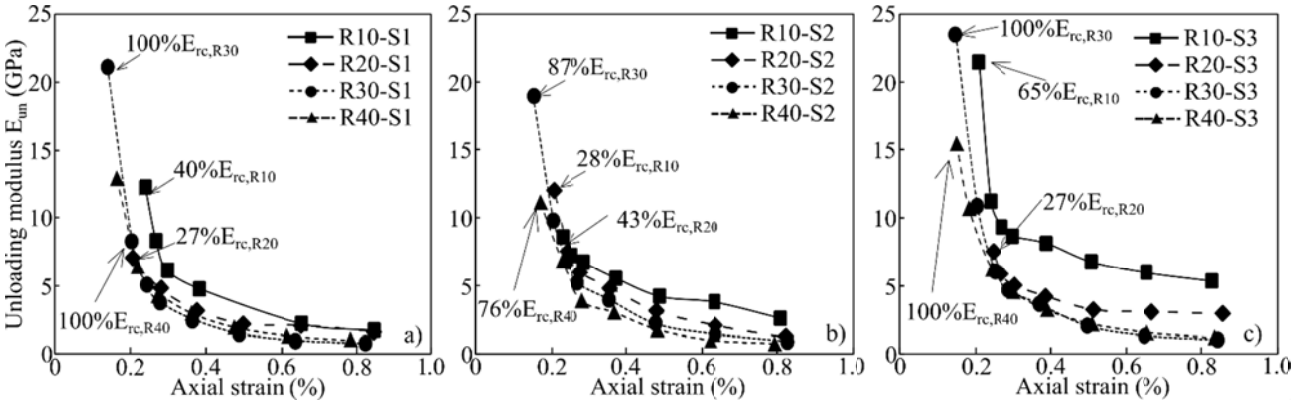

Figure 11 Effect of rubber content on the unloading stiffness E_{un} of RuC loaded under different strain rates: a) S1, b) S2, c) S3

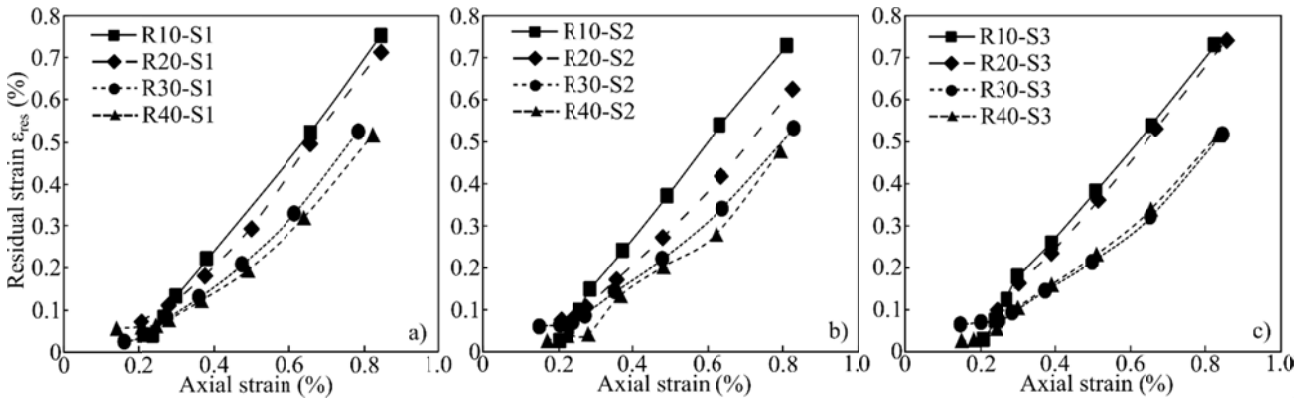

Figure 12 Effect of rubber content on the residual strain ε_{res} of RuC loaded under different strain rates: a) S1, b) S2, c) S3

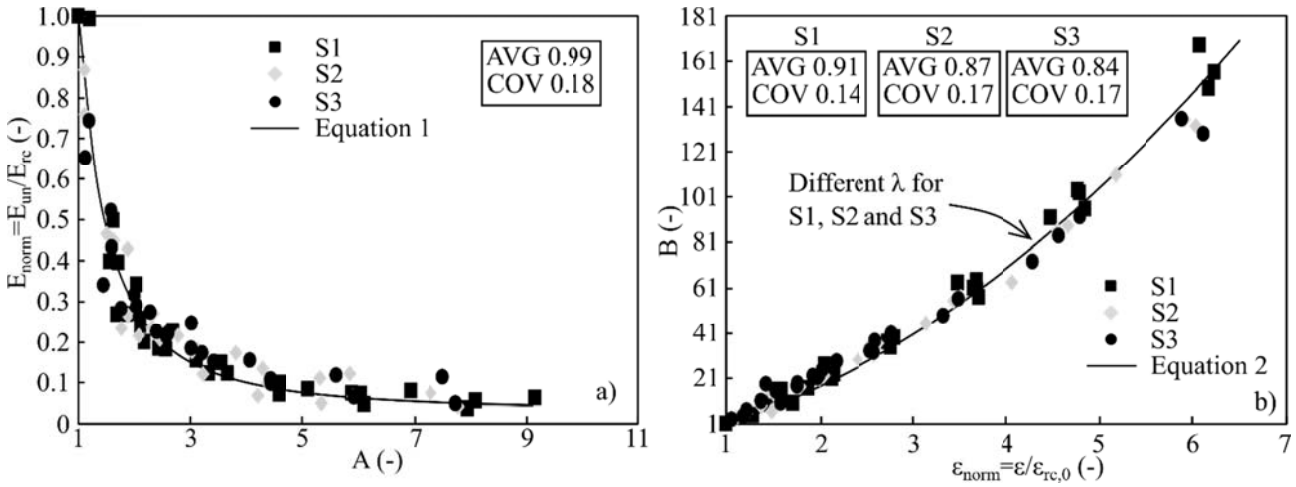

Figure 13 Proposed assessment expressions for: a) unloading stiffness and b) residual strain

Tables

Table 1 Sieve analysis

Sieves of square aperture (mm)	Passing Percentage %			
	Rubber 0.5-0.8	Rubber 1.0-2.5	Sand	Gravel
0	0	0	0	0
0.15	0.06	0.02	2.43	0.39
0.30	0.23	0.02	24.0	1.06
0.60	0.42	0.10	64.9	1.95
1.25	99.7	8.82	84.7	2.95
2.50	99.9	99.1	91.7	4.71
5.00	100	100	97.6	16.1
10.0	100	100	100	85.5
14.0	100	100	100	99.5
20.0	100	100	100	100

Table 2 Concrete mix designs

		R00	R10	R20	R30	R40
Binders (kg/m3)	Cement	225	225	225	225	225
	Fly ash	158	158	158	158	158
	Silica fume	67	67	67	67	67
Aggregates (kg/m3)	Sand (0-5 mm)	760	681	602	524	445
	Gravel (10-20 mm)	977	876	774	673	572
Rubber (kg/m3)	0.5-0.8 mm	0	24	48	72	96
	1.0-2.5 mm	0	31	62	93	124
Admixture (L/m3)		9.5	9.5	9.5	9.5	9.5
w/c		0.35	0.35	0.35	0.35	0.35

Table 3* Mechanical properties of RuC and CCM materials

Specimen	Rubber content ρ_{rv}	Strain rate $\dot{\varepsilon}$ (sec^{-1})	Monotonic properties				Cyclic properties			
			f_{rc} (MPa)	E_{rc} (GPa)	$\varepsilon_{rc,0}$ (‰)	G_{cl} (N/mm^2)	f_{rc} (MPa)	E_{rc} (GPa)	$\varepsilon_{rc,0}$ (‰)	G_{cl} (N/mm^2)
R00-S1	0	1.67×10^{-5}	82.7±2.7	40.0±3.1	2.164±0.035	0	79.0±3.8	39.1±0.3	2.043±0.153	0
R00-S2		1.67×10^{-3}	88.8±4.1	41.6±1.4	2.173±0.096	0	91.1±1.7	40.2±0.9	2.248±0.045	0
R00-S3		1.67×10^{-2}	96.0±4.0	43.4±0.3	2.265±0.084	0	95.6±1.2	40.5±1.6	2.343±0.011	0
R10-S1	0.1	1.67×10^{-5}	58.1±5.4	30.5±0.1	1.886±0.020	0.068	55.5±0.7	30.5±4.1	1.900±0.289	0.053
R10-S2		1.67×10^{-3}	67.0±5.0	32.6±1.2	1.948±0.140	0.080	63.1±1.8	31.2±0.4	2.100±0.100	0.067
R10-S3		1.67×10^{-2}	67.2±4.8	36.0±0.5	1.991±0.306	0.057	62.8±6.2	32.9±0.9	1.967±0.208	0.044
R20-S1	0.2	1.67×10^{-5}	36.3±3.2	25.9±2.7	1.368±0.134	0.040	36.3±1.5	26.2±1.1	1.473±0.265	0.042
R20-S2		1.67×10^{-3}	39.2±3.9	30.6±0.6	1.426±0.099	0.041	36.4±2.7	27.9±0.7	1.367±0.058	0.052
R20-S3		1.67×10^{-2}	42.0±3.8	33.8±3.3	1.441±0.020	0.044	37.1±3.9	27.4±0.7	1.400±0.141	0.049
R30-S1	0.3	1.67×10^{-5}	25.9±1.5	21.5±0.9	1.320±0.096	0.037	25.8±1.9	20.6±0.6	1.362±0.115	0.039
R30-S2		1.67×10^{-3}	29.5±1.5	22.0±1.2	1.393±0.084	0.046	28.7±1.3	21.9±0.3	1.400±0.003	0.040
R30-S3		1.67×10^{-2}	32.4±0.9	24.3±0.2	1.582±0.031	0.049	29.2±1.8	20.8±1.9	1.433±0.058	0.050
R40-S1	0.4	1.67×10^{-5}	17.8±1.1	15.7±1.0	1.290±0.091	0.038	18.4±2.5	13.1±1.4	1.378±0.071	0.030
R40-S2		1.67×10^{-3}	20.6±2.5	15.5±0.2	1.503±0.046	0.047	20.3±2.1	14.6±2.4	1.533±0.058	0.041
R40-S3		1.67×10^{-2}	21.1±3.3	14.6±2.0	1.588±0.388	0.051	20.2±2.3	14.4±0.7	1.533±0.058	0.040

* Results listed in the table are the average values of 3 test results of each specimen reference.